PNAS RESEARCH ARTICLE | CELL BIOLOGY

Lysosome-related organelles contain an expansion compartment that mediates delivery of zinc transporters to promote homeostasis

Adelita D. Mendoza[a,1,2], Nicholas Dietrich[a,1,3], Chieh-Hsiang Tan[a,4], Daniel Herrera[a], Jennysue Kasiah[a], Zachary Payne[a], Ciro Cubillas[a], Daniel L. Schneider[a], and Kerry Kornfeld[a]

Edited by Mary Lou Guerinot, Dartmouth College, Hanover, NH; received May 4, 2023; accepted November 22, 2023

Zinc is an essential nutrient—it is stored during periods of excess to promote detoxification and released during periods of deficiency to sustain function. Lysosome-related organelles (LROs) are an evolutionarily conserved site of zinc storage, but mechanisms that control the directional zinc flow necessary for homeostasis are not well understood. In *Caenorhabditis elegans* intestinal cells, the CDF-2 transporter stores zinc in LROs during excess. Here, we identify ZIPT-2.3 as the transporter that releases zinc during deficiency; ZIPT-2.3 transports zinc, localizes to the membrane of LROs in intestinal cells, and is necessary for zinc release from LROs and survival during zinc deficiency. In zinc excess and deficiency, the expression levels of CDF-2 and ZIPT-2.3 are reciprocally regulated at the level of mRNA and protein, establishing a fundamental mechanism for directional flow to promote homeostasis. To elucidate how the ratio of CDF-2 and ZIPT-2.3 is altered, we used super-resolution microscopy to demonstrate that LROs are composed of a spherical acidified compartment and a hemispherical expansion compartment. The expansion compartment increases in volume during zinc excess and deficiency. These results identify the expansion compartment as an unexpected structural feature of LROs that facilitates rapid transitions in the composition of zinc transporters to mediate homeostasis, likely minimizing the disturbance to the acidified compartment.

zinc homeostasis | lysosome | expansion compartment | zinc transporters | *C. elegans*

Significance

Zinc homeostasis is important for human health. When zinc homeostasis becomes dysregulated, human pathologies arise. LROs (Lysosome-related organelles) are key sites for macromolecule degradation and zinc trafficking. CDF-2 and ZIPT-2.3 localize to LROs and their expression levels are reciprocally regulated by zinc. LROs contain an acidified compartment and an expansion compartment—they are not simply a sphere with a single lipid bilayer but are structurally more complex. The expansion compartment increases in volume in zinc excess and deficiency, demonstrating that LRO morphology is dynamic. CDF-2 localizes to both compartments, whereas ZIPT-2.3 localizes to the acidified compartment only. This distribution of zinc transporters and dynamic LRO morphology permits rapid delivery of zinc transporters and directional movement of zinc to promote homeostasis.

Zinc is essential for all organisms, playing a wide range of structural (1), catalytic (2), and signaling roles (3); it is predicted to bind ~10% of the human proteome (4). Because deficiency and excess are deleterious, zinc levels are regulated by homeostatic mechanisms (5). Zinc homeostasis occurs in individual cells and whole organisms, and integration of cellular and organismal zinc homeostasis is not well defined. Transmembrane proteins that transport zinc across cellular membranes are key elements of zinc homeostasis; SLC30A/ZNT/CDF family proteins reduce cytosolic zinc levels by transporting zinc from cytosol to extracellular spaces or organelle lumens, whereas SLC39A/Zrt,Irt-like (ZIP) family proteins increase cytosolic zinc levels by transporting zinc in the opposite directions (6).

Caenorhabditis elegans is a useful and relevant model system to study zinc homeostasis due to powerful genetic approaches, a transparent body that facilitates imaging, and conservation of CDF and ZIP transporters (7, 8). HIZR-1, the high-zinc sensor and master regulator of high-zinc homeostasis, is a nuclear receptor transcription factor composed of a ligand-binding domain (LBD) and a DNA-binding domain (DBD) (9). When zinc binds the LBD, HIZR-1 translocates to the nucleus and directly binds a DNA enhancer called the High Zinc Activation (HZA) element (10). HIZR-1 bound to the HZA recruits the mediator complex and RNA polymerase to activate transcription of multiple genes that promote high zinc homeostasis (11, 12). One direct target is *cdf-2;* CDF-2 transports zinc from the cytosol to the lumen of lysosome-related organelles (LROs) in intestinal cells, also called gut granules, to detoxify and store zinc (13).

In zinc-replete conditions, LROs were spherical and labeled with LysoTracker, which stains acidified compartments. Roh et al. (2012) reported that LROs change shape in excess zinc, displaying a bilobed morphology; CDF-2 localizes to both lobes, whereas LysoTracker stains only one lobe (13). The discovery that LROs change morphology in excess zinc raised new questions: What is the mechanism of LRO shape change? What is the structure and function of each lobe? Where is the zinc stored? How does the bilobe structure promote high zinc homeostasis?

The low-zinc homeostasis pathway in *C. elegans* is beginning to be described (7, 8). *zipt-2.1*, *zipt-2.3*, and *zipt-7.1* display increased levels of mRNA during zinc deficiency (14); promoters of these genes contain low zinc activation (LZA) elements that promote transcriptional activation during zinc deficiency. These results suggest an LZA-binding protein, yet to be

Copyright © 2024 the Author(s). Published by PNAS. This article is distributed under Creative Commons Attribution-NonCommercial-NoDerivatives License 4.0 (CC BY-NC-ND).

[1]A.D.M. and N.D. contributed equally to this work.

[2]To whom correspondence may be addressed. Email: adelitadmendoza@wustl.edu.

[3]Present address: Epigenetics and Stem Cell Biology Laboratory, National Institute of Environmental Health Sciences, NIH, NC 27709.

[4]Present address: Division of Biology and Biological Engineering, California Institute of Technology, Pasadena, CA 91125.

This article contains supporting information online at https://www.pnas.org/lookup/suppl/doi:10.1073/pnas.2307143121/-/DCSupplemental.

Published February 8, 2024.

defined, may function as a low-zinc sensor, and these *zipt* genes may promote low-zinc homeostasis. While CDF-2 transports zinc into the lumen of LROs during zinc excess, the mechanism of zinc release during zinc deficiency has yet to be defined.

Here, we show that ZIPT-2.3 specifically localizes to the membrane of LROs and promotes zinc release during deficiency. *zipt-2.3* transcription is activated during zinc deficiency and repressed during zinc excess. CDF-2 is reciprocally regulated at the mRNA and protein levels, and we propose that reciprocal regulation of CDF-2 and ZIPT-2.3 protein levels on the membrane of LROs is a fundamental mechanism of homeostasis and the key to directional flow of zinc. Super-resolution microscopy revealed that LROs consist of two compartments: an acidified compartment and an expansion compartment. Labile zinc is concentrated in the acidified compartment, which contains both CDF-2 and ZIPT-2.3. The expansion compartment is present in all zinc conditions; it is contracted in zinc-replete conditions, and it increases in volume dramatically in zinc excess and moderately in zinc deficiency, suggesting that increased volume is a response to high and low-zinc homeostasis. The expansion compartment appears to grow by vesicular fusion, suggesting that it functions to mediate delivery of zinc transporters; this may be a mechanism to alter the ratio of transporters without disturbing the acidified compartment. These results provide a high-resolution view of a dynamic compartment that is an integral part of LROs.

Results

ZIPT-2.3 Is a Zinc Transporter Localized to LROs in Intestinal Cells. Fourteen *C. elegans* genes encode ZIP family proteins, named *zipt* genes (14, 15). Three of these, *zipt-2.1*, *zipt-2.3,* and *zipt-7.1*, contain LZA enhancers and are transcriptionally activated during zinc deficiency, suggesting that these genes play roles in zinc homeostasis (14). To further explore regulation, we analyzed transcript levels of *zipt* genes in zinc excess. *zipt-2.3* mRNA levels were significantly lower in excess zinc. This is a specific regulatory response, since 13 other *zipt* genes did not display significant regulation (*SI Appendix*, Fig. S1*I*). Because it is regulated in zinc deficiency and excess, we focused on *zipt-2.3*, which includes five exons and generates an 1,108 nucleotide mRNA (Fig. 1*A*). The ZIPT-2.3 protein is highly similar to *Homo sapiens* ZIP2, *Drosophila melanogaster* dZip (16), and *Danio rerio Dr*ZIP1 (17), suggesting that genes encoding these proteins derived from a common ancestral gene (*SI Appendix*, Fig. S2*A*).

Many ZIP proteins transport zinc, but some transport iron or other metals (18). To investigate the ability of ZIPT-2.3 to transport zinc, we expressed ZIPT-2.3 by transient transfection in human embryonic kidney cells (HEK293T) and determined the rate of uptake using radioactive zinc (19). Control cells displayed baseline uptake mediated by endogenous zinc transporters; cells expressing ZIPT-2.3 displayed a significant increase ($P < 0.0001$)

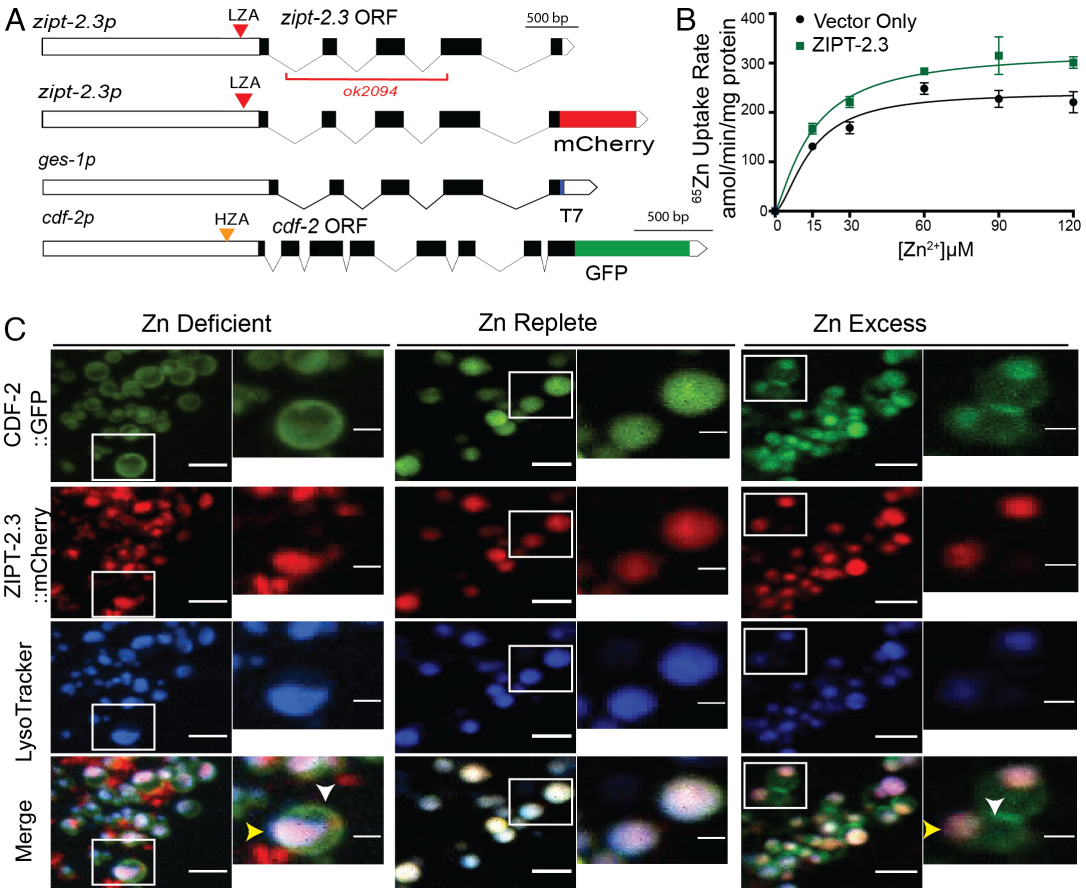

Fig. 1. ZIPT-2.3 is a zinc transporter that localizes to LROs. (*A*) Diagrams show a portion of the plasmids in transgenic strains that express *zipt-2.3* or *cdf-2*. White boxes represent promoter and 3′ UTR regions, black boxes and lines represent coding regions and introns. Red, blue, and green coding regions represent mCherry, T7, and GFP, respectively. Triangles represent LZA (red) and HZA (orange) enhancers. The red line indicates the extent of the *ok2094* deletion mutation. (*B*) Human HEK293T cells expressing ZIPT-2.3 or a vector control were incubated with various concentrations of zinc containing a fixed fraction of radioactive ^{65}Zn. The rate of zinc uptake was determined by measuring radioactivity that accumulated in the cells. Values are mean and SE (N = 4 experimental replicates) evaluated by 2-way ANOVA (****$P < 0.0001$). (*C*) Transgenic animals expressing CDF-2::GFP (green) and ZIPT-2.3::mCherry (red) were cultured with LysoTracker Blue in zinc replete, excess, or deficient conditions for 16 h and visualized with confocal microscopy. Yellow arrowheads indicate acidifed compartment; white arrowheads indicate expansion compartment. Scale bars, 5 µm in larger image, and 1 µm in smaller *Inset* indicated by white box.

in zinc uptake (Fig. 1*B*). Thus, ZIPT-2.3 was sufficient to promote zinc uptake, consistent with the model that ZIPT-2.3 is a physiological zinc transporter (*SI Appendix*, Fig. S2*B*). These data are also consistent with the model that ZIPT-2.3 enhances the uptake of endogenous zinc transporters. Because zinc uptake in transfected cells is mediated by a combination of endogeonous transporters and ZIPT-2.3, we did not attempt to use these data to determine the kinetic parameters of ZIPT-2.3 such as Km and Vmax.

To determine the localization of ZIPT-2.3, we generated transgenic animals expressing the *zipt-2.3* promoter and coding region fused to the coding region of mCherry (Fig. 1*A*). A double colon (::) indicates fusion proteins. This ZIPT-2.3::mCherry protein is functional, since expression in transgenic animals rescued the *zipt-2.3(lf)* phenotype of reduced growth in zinc deficiency (*SI Appendix*, Fig. S2*C*). Using spinning disk confocal microscopy, transgenic animals cultured in zinc-replete medium displayed a punctate pattern of expression in intestinal cells, suggestive of localization to LROs (Fig. 1*C*); Chapman et al. (2019) reported a similar localization pattern and identified a role for *zipt-2.3* in germline apoptosis (20). To characterize this punctate pattern, we used LysoTracker, a dye that stains acidified lysosomes. ZIPT-2.3::mCherry colocalized with LysoTracker, indicating that ZIPT-2.3 localizes to the membrane of acidified LROs in intestinal cells (Fig. 1*C*).

In excess zinc, intestinal LROs are the major site of zinc storage; the CDF-2 transporter localizes to these organelles and promotes zinc storage (13, 21). To examine colocalization, we generated transgenic animals that express CDF-2::GFP and ZIPT-2.3::mCherry (Fig. 1*A*). In a zinc-replete medium, LROs appeared spherical, and CDF-2::GFP and ZIPT-2.3::mCherry displayed complete colocalization (Fig. 1 *C*, *Middle*). In excess zinc, many LROs displayed a bilobed morphology; CDF-2::GFP was localized to the membrane of both lobes, whereas ZIPT-2.3::mCherry and LysoTracker were only localized to one lobe (Fig. 1 *C*, *Right*). To examine zinc deficiency, we cultured animals with the zinc chelator N,N,N′,N′-Tetrakis (2-pyridylmethyl)ethylenediamine (TPEN). In zinc deficiency, LROs displayed a LysoTracker positive lobe that contains CDF-2 and ZIPT-2.3 and a small LysoTracker negative lobe that contains CDF-2 but not ZIPT-2.3 (Fig. 1 *C*, *Left*). Thus, LROs in intestinal cells are spherical in zinc-replete conditions and remodeled during zinc excess and deficiency; in both zinc extremes, a LysoTracker positive lobe contains CDF-2 and ZIPT-2.3 while a LysoTracker negative lobe contains CDF-2 but not ZIPT-2.3.

Genetic Analysis Demonstrates that *zipt-2.3* Promotes Mobilization of Zinc from LROs and Influences Cytosolic Levels of Zinc. Based on the localization and transport activity of ZIPT-2.3, we predicted that a *zipt-2.3* loss-of-function*(lf)* mutant would be defective in mobilizing zinc stored in LROs. To test this prediction, we analyzed the *ok2094* mutation that removes 1,561 base pairs of *zipt-2.3*, including all of exons 2 and 3 and part of exon 4 (Fig. 1*A*). These exons encode highly conserved regions of the protein, suggesting *zipt-2.3(ok2094)* is a strong loss-of-function or null allele. We used an established assay based on localization of the zinc dye FluoZin-3 AM to LROs (13). Wild-type and *zipt-2.3(lf)* animals cultured with supplemental zinc and FluoZin-3 AM for 16 h displayed strong fluorescence in LROs, indicating robust zinc storage (Fig. 2*A*). When shifted to zinc-replete or -deficient conditions, wild-type animals displayed a significant decrease in fluorescence after 24 or 48 h, indicating that stored zinc is mobilized from LROs. By contrast, *zipt-2.3(lf)* animals did not display reduced fluorescence, indicating a failure to mobilize stored zinc (Fig. 2 *A*–*C*). Thus, ZIPT-2.3 was necessary to mobilize zinc from intestinal LROs.

If ZIPT-2.3 releases stored zinc, then we predict that *zipt-2.3(lf)* mutants will have lower levels of cytosolic zinc compared to wild type. To test this prediction, we analyzed the expression levels of zinc-regulated genes as a surrogate marker for cytosolic zinc levels.*zipt-2.1* and *F44E7.5* are activated by zinc-deficient conditions (14); the mRNA levels of both genes were increased significantly in *zipt-2.3(lf)* mutant animals compared to wild type, suggesting cytosolic zinc levels are decreased in these mutant animals (Fig. 2*D*). To determine if *zipt-2.3* is sufficient to increase cytosolic zinc levels, we overexpressed *zipt-2.3* in intestinal cells. We generated a transgenic strain containing multiple copies of *zipt-2.3* controlled by the ges-1 promoter (*zipt-2.3*(*oe*)) that is constitutively expressed in intestinal cells (Fig. 1*A*). *mtl-1* and *cdf-2* are activated by zinc-excess conditions (21), and the mRNA levels of both genes were increased significantly in *zipt-2.3*(*oe*) mutant animals compared to wild type, suggesting cytoplasmic zinc levels are increased in these mutant animals (Fig. 2*E*). Thus, *zipt-2.3* was necessary to release stored zinc and maintain normal levels of cytosolic zinc and sufficient to increase cytosolic zinc levels.

***zipt-2.3* Promotes Organismal Zinc Homeostasis.** To investigate the function of *zipt-2.3* in organismal zinc homeostasis, we analyzed the growth rate of wild-type and *zipt-2.3(lf)* animals in zinc deficiency. Synchronized L1 stage animals were cultured for 72 h, and length was determined as a quantitative measure of growth (13). In a zinc-replete medium, wild-type and *zipt-2.3(lf)* animals grew and developed to similar-sized adults. In zinc deficiency, wild-type animals displayed a slight, dose-dependent growth inhibition. By contrast, *zipt-2.3(lf)* mutants displayed severe growth defects, indicating hypersensitivity to zinc deficiency (Fig. 3*A*). Mutations of six other *zipt* genes did not cause hypersensitivity, suggesting that this phenotype is specific (*SI Appendix*, Fig. S1 *C*–*H*). Furthermore, *zipt-2.3(lf)* animals did not display hypersensitivity to the iron chelator 2,2-bipyridyl or the manganese chelator diaminocyclohexanetetraacetic acid, indicating that the phenotype is specific for zinc deficiency (Fig. 3*B* and *SI Appendix*, Fig. S1*B*). *zipt-2.3(oe)* animals displayed hypersensitivity to excess zinc compared to wild type (Fig. 3*C*). Thus, *zipt-2.3* was necessary for growth and development in zinc deficiency and sufficient to cause hypersensitivity to high zinc toxicity.

The CDF-2 protein promotes storage during zinc excess; *cdf-2(lf)* mutant animals displayed hypersensitivity to growth defects caused by excess zinc but displayed normal growth in zinc deficiency (Fig. 3*D*). By contrast, *zipt-2.3(lf)* animals displayed hypersensitivity to growth defects caused by zinc deficiency but displayed normal growth in zinc excess (Fig. 3*E*). Roh et al. (2012) showed that loss-of-function mutations in LRO biogenesis genes *glo-1*, *pgp-2*, and *glo-3* reduced intestinal zinc levels, suggesting that zinc is stored in these LROs (13). *glo-1* enodes a Rab GTPase that localizes to LROs. To test the prediction that intestinal LROs themselves function in zinc homeostasis, we analyzed growth of *glo-1(zu391)* mutant animals in zinc excess and deficiency (22). *glo-1(lf)* animals were hypersensitive to growth defects caused by zinc deficiency and excess, consistent with the model that intestinal LROs play a central role in zinc homeostasis (Fig. 3*F*). An alternative interpretation is that *glo-1* mutants have other defects that impair growth in zinc extremes. The *glo-1* gene may have multiple functions including protein trafficking to LROs, LRO biogenesis, and assembly (22, 23). GLO-1 also participates in protein trafficking to LROs, but it requires WHT-2, an ABC transporter, to localize to LROs (24).

Wild-type animals exposed to excess zinc early in life display resistance to growth defects caused by zinc deficiency later in life, presumably because they mobilize stored zinc (*SI Appendix*,

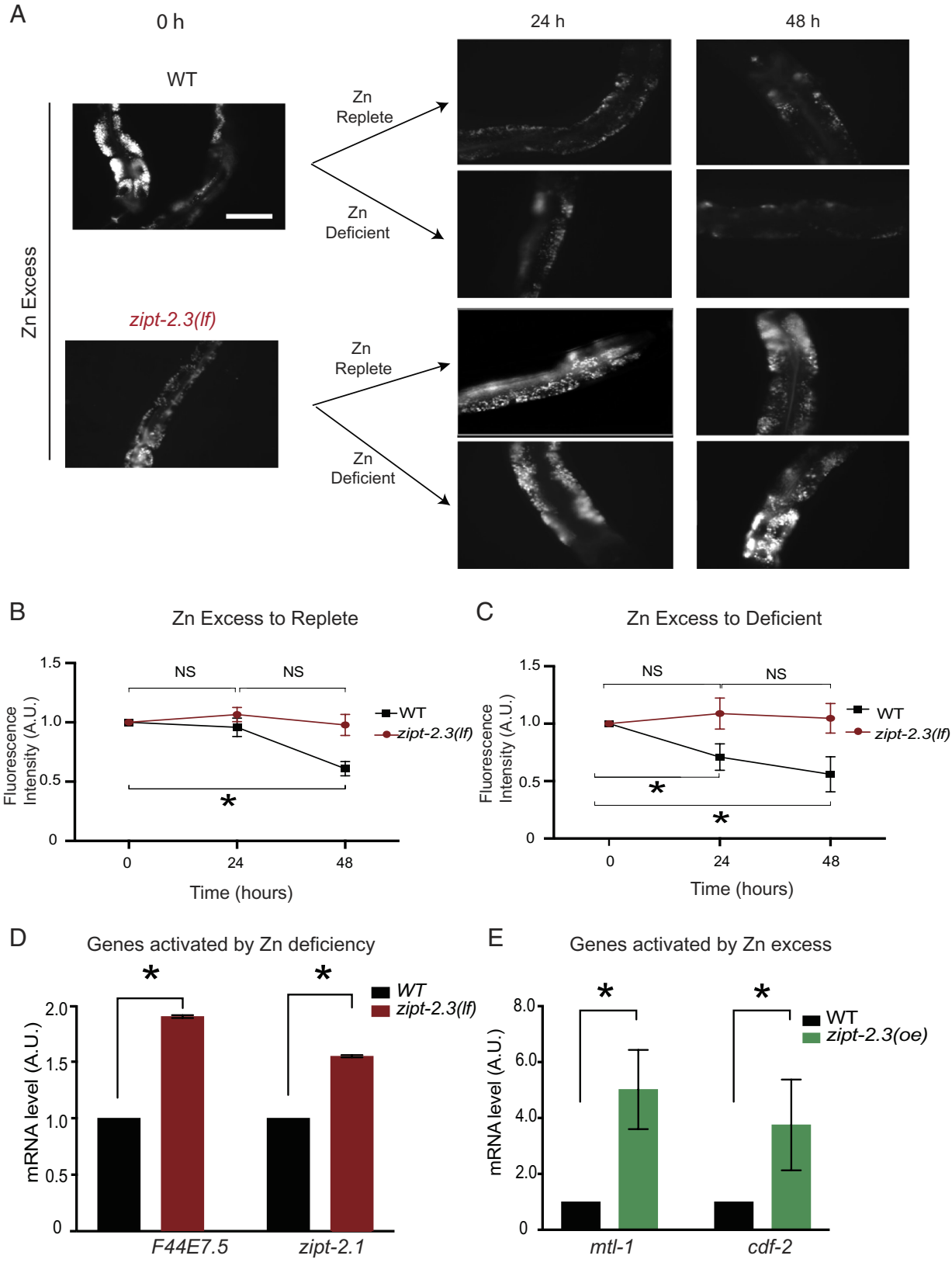

Fig. 2. ZIPT-2.3 transports zinc from the lumen of LROs to the cytosol. (*A*) Wild-type and *zipt-2.3(ok2094)* animals were cultured with 200 μM supplemental zinc to promote zinc storage and FluoZin-3 AM to visualize labile zinc in LROs in intestinal cells. Animals were transferred to zinc-replete or zinc-deficient medium (200 μM TPEN), and FluoZin-3 AM fluorescence was analyzed by microscopy after 24 and 48 h. Representative fluorescence images show a portion of the intestine; white displays FluoZin-3 AM fluorescence. (*B* and *C*) Quantification of fluorescence intensity: the value at time 0 was set to 1.0 arbitrary units (AU), and other values were normalized. Values are the average of three biological replicates ± SD (*$P < 0.05$). (*D* and *E*) Populations of mixed-stage, wild-type, *zipt-2.3(ok2094), or amEx350* [*zipt-2.3(oe)*] animals were cultured in standard zinc-replete conditions. RNA was analyzed by qPCR. The value for WT was set to 1.0 arbitrary units (AU) for each gene, and mutant values were normalized. One dish of worms is a biological replicate; values are the average of 3 biological replicates and the SD (*$P < 0.05$).

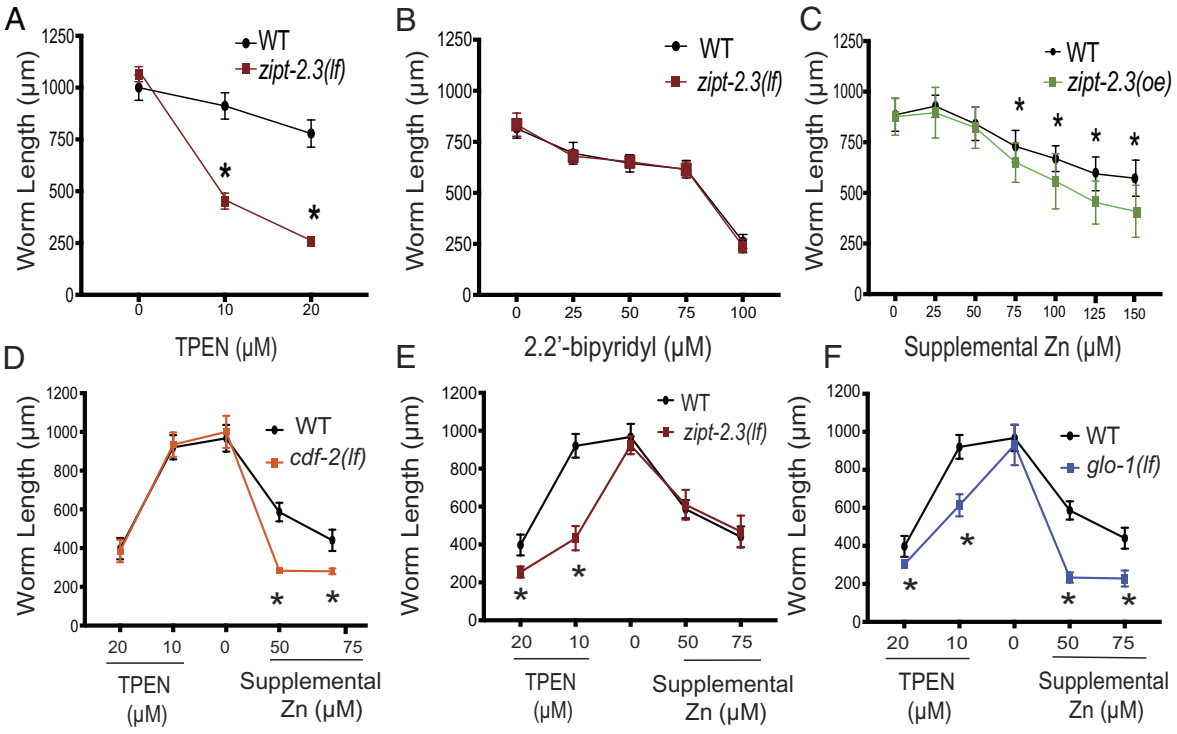

Fig. 3. *zipt-2.3*, *cdf-2*, and *glo-1* function in organismal zinc homeostasis. (*A–F*) L1 larvae were cultured on standard NAMM dishes or dishes containing the zinc chelator TPEN, the iron chelator 2,2′-bipyridyl, or supplemental zinc for 3 d, and the length of individual worms was measured. Genotypes: *zipt-2.3(ok2094)*, *amEx350* [*zipt-2.3(oe)*], *cdf-2(tm788)*, *glo-1(zu391)*, and wild type. Values represent the average length ± SD (3 independent biological replicates, **P* < 0.05). [*A*, WT = 51 worms, *zipt-2.3(lf)* = 61 worms; *B*, WT = 180 worms, *zipt-2.3(lf)* = 160 worms; *C*, WT = 215 worms, *zipt-2.3(oe)* = 166 worms; *D*, WT = 119 worms, *cdf-2(lf)* = 88 worms; *E*, WT = 119 worms, *zipt-2.3(lf)* = 134 worms; *F*, WT = 119 worms, *glo-1(lf)* = 72 worms].

Fig. S1*I*) (13). We predicted that *zipt-2.3* is necessary to utilize stored zinc. Consistent with this prediction, *zipt-2.3(lf)* mutants did not display increased resistance when exposed to excess zinc early in life (*SI Appendix*, Fig. S1*J*). *glo-1(lf)* mutants displayed a similar defect, consistent with the central role of LROs in zinc storage and release (*SI Appendix*, Fig. S1*K*).

Reciprocal Regulation of ZIPT-2.3 and CDF-2 Mediates Zinc Homeostasis. *cdf-2* mRNA levels increase in excess zinc, and *zipt-2.3* mRNA levels increase in zinc deficiency (13, 14). To further analyze regulatory control, we cultured wild-type animals for 16 h with 40 μM TPEN (zinc deficient), 200 μM supplemental zinc (zinc excess), or no supplemental zinc or TPEN (zinc replete) and analyzed mRNA levels. In zinc deficiency, the level of *zipt-2.3* mRNA increased significantly and the level of *cdf-2* mRNA decreased significantly compared to replete conditions. By contrast, in zinc excess, the level of *zipt-2.3* mRNA decreased significantly and the level of *cdf-2* mRNA increased significantly compared to replete conditions (Fig. 4*A*). Fluorescence imaging with transgenic animals containing CDF-2::GFP and ZIPT-2.3::mCherry fusion proteins showed reciprocal regulatory control was also observed at the level of protein expression (Fig. 4*B*). These results suggest a mechanism for directional flow of zinc from the cytosol into the lumen of LROs during excess, when CDF-2 levels are high and ZIPT-2.3 levels are low, and from the lumen of LROs back into the cytosol during deficiency, when ZIPT-2.3 levels are high and CDF-2 levels are low.

Super-Resolution Microscopy Reveals that LROs Are Composed of an Acidified Compartment and an Expansion Compartment. To define mechanisms that promote dynamic changes in the composition of zinc transporters on the membranes of LROs, we observed individual organelles at 120 nm resolution using super-resolution microscopy. Animals raised in zinc-replete medium were transferred to zinc deficient, replete, or excess conditions for 16 h and visualized with three different fluorescent markers. One strain expressed CDF-2::GFP and ZIPT-2.3::mCherry and was stained with LysoTracker (Fig. 5 *A–D* and *SI Appendix*, Figs. S3 and S6–S8) (25). The second strain expressed CDF-2::mCherry and was stained with LysoTracker and FluoZin-3 AM, which stains labile zinc (Fig. 5 *E–H* and *SI Appendix*, Figs. S4 and S9–S11). Individual organelles that did not overlap neighboring organelles were reconstructed in three dimensions, and maximum-intensity projections (MIP) were prepared. The MIP is a composite of all planes of a z-stack obtained during imaging and thus represents the entire LRO. For clarity of presentation, we applied an arbitrary color for each marker: CDF-2 is red, ZIPT-2.3 is green, LysoTracker is blue, and labile zinc is yellow (Figs. 5–7).

To define relationships between the markers, we performed line scans on each LRO. Because each color represents a different molecule, it is not informative to compare the relative intensities of colors. Therefore, each of the three colors was normalized to a maximum value of 1.0 (Fig. 5 *B–D* and *F–H* and *SI Appendix*, Figs. S6–S11). The interpretation of the line scans revealed that LROs are composed of two compartments in all zinc conditions: an **acidified compartment** that stains with LysoTracker, and an **expansion compartment** that is LysoTracker negative. We assigned names to compartments, regions, and membranes (labeled in bold). The **acidified compartment membrane** contains both CDF-2 and ZIPT-2.3 and surrounds the spherical acidified compartment. The acidified compartment has two regions—the **LysoTracker region** forms the center of the sphere and stains strongly with LysoTracker and weakly with FluoZin-3 AM, whereas the **zinc region** forms the periphery of the sphere and stains strongly with FluoZin-3 AM and weakly

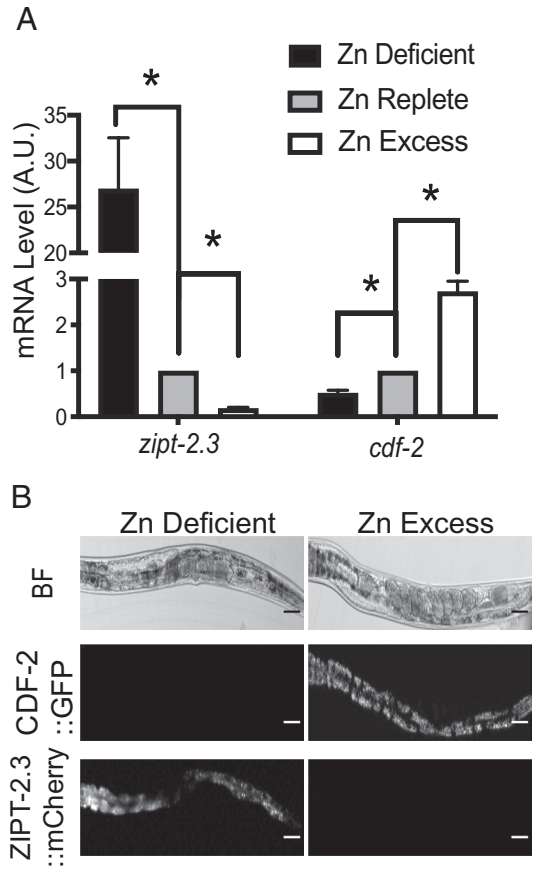

Fig. 4. Zinc reciprocally regulates *zipt-2.3* and *cdf-2* mRNA levels, and ZIPT-2.3 and CDF-2 protein levels. (*A*) A population of mixed-stage, wild-type animals were cultured with 200 μM supplemental zinc (zinc excess), 40 μM TPEN (zinc deficient), or standard medium (zinc replete) for 16 h. RNA was analyzed by qPCR. The value in zinc-replete conditions was set equal to 1.0 arbitrary units (AU), and other values normalized. One dish of worms is a biological replicate; average of 3 biological replicates ± SD. (*B*) Transgenic L4 stage larvae expressing CDF-2::GFP and ZIPT-2.3::mCherry were cultured with 50 μM TPEN or 200 μM supplemental zinc for 16 h. Representative images show one worm with bright field (BF, *Upper*), green fluorescence (*Middle*), or red fluorescence (*Lower*). White indicates protein expression in intestinal cells. (Scale bar, 10 μm.)

with LysoTracker. The zinc region appears as a crescent adjacent to the interface membrane in zinc excess. The expansion compartment is a hemisphere that is dynamic in shape and volume. The **expansion compartment membrane** contains CDF-2 but not ZIPT-2.3 and appears to attach with or surround the acidified compartment membrane. The expansion and acidified compartments appear to be separated by a portion of the acidified compartment membrane that we named the **interface membrane**. Fig. 6*A* shows a diagram of an LRO in excess zinc.

The Expansion Compartment Increases in Volume in Response to Zinc Excess and Deficiency. To characterize remodeling in response to changes in zinc levels, we quantified compartment volumes. Volumes were calculated by assuming that the compartments were spheres, hollow spheres, or hemispherical segments, based on our microscope images (*SI Appendix*, Fig. S5). In zinc-replete conditions, LROs are approximately spherical with a total average volume of ~7.6 μm^3 (Fig. 6*D*). The acidified compartment represents 83% of the total volume, with a large LysoTracker region (~5.9 μm^3) and a small zinc region (~0.6 μm^3). The expansion compartment is contracted; its volume of ~1.2 μm^3 represents 17% of the total volume (Fig. 6 *B* and *D*). Although contracted, the expansion compartment can be visualized with super-resolution microscopy in zinc-replete conditions (Fig. 5 *A* and *C* and *SI Appendix*, Figs. S3*B* and S4*B*). In many cases, the line scan reveals the CDF-2 boundary (red line) is outside the ZIPT-2.3 boundary (green line), indicating the line scan passes through the expansion compartment membrane before passing through the acidified compartment membrane (Fig. 5*C*). The ZIPT-2.3 membrane coincides closely with LysoTracker (*SI Appendix*, Fig. S3). The LysoTracker and FluoZin-3 AM staining overlap extensively, and there is frequently a small zinc region outside the LysoTracker boundary (Fig. 5*G*). Overall, LROs in zinc-replete medium appear to have stable membrane dynamics, store a small amount of zinc, and have a prominent acidified compartment.

After 16 h in zinc excess, LROs increase in total volume about 60% to an average of ~12.0 μm^3 (Figs. 5 *D* and *H* and 6 *C* and *D* and *SI Appendix*, Fig. S12*E*). The prominent expansion compartment is shaped like a hemisphere and increases about eightfold to ~9.3 μm^3; this represents 76% of the total volume. The acidified compartment is spherical and shrinks overall to 2.7 μm^3- 24% of total volume; the LysoTracker region is 1.8 μm^3, while the zinc region is ~0.9 μm^3 (Fig. 6 *B* and *D* and *SI Appendix*, Fig. S12). In most cases, the line scans reveal that the CDF-2 boundary (red line) is coincident with the ZIPT-2.3 boundary (green line) as it passes through the acidified compartment membrane (Fig. 5 *A* and *D* and *SI Appendix*, Fig. S8). In most cases, there is a distinct zinc region shaped like a crescent: Line scans reveal FluoZin-3 AM staining extends beyond the LysoTracker stain and is coincident with the CDF-2 membrane, indicating that the crescent of zinc is located in the acidified compartment rather than the expansion compartment (Fig. 5 *E* and *H*). Overall, LROs in zinc excess appear to have active membrane dynamics driving a growing expansion compartment and a prominent crescent of zinc staining localized to the acidified compartment.

After 16 h in zinc deficiency, LROs increase slightly to a total average volume of ~8.3 μm^3 (Figs. 5 *B* and *F* and 6 *B* and *D*). An expansion compartment shaped like a hemisphere is frequently visible with an average volume of ~2.0 μm^3; this is about 60% larger than in replete conditions, representing 25% of total volume of the organelle. The acidified compartment is ~6.3 μm^3, which is 75% of total volume; the LysoTracker region is ~5.3 μm^3 while the zinc region is ~1.0 μm^3 (Fig. 6*D* and *SI Appendix*, Fig. S12). Overall, LROs in zinc deficiency appear to have active membrane dynamics leading to a larger expansion compartment and a mostly unchanged acidified compartment.

In excess zinc, the volume of LROs varied ~15-fold; of eleven analyzed in detail, the smallest was ~2.2 μm^3 and the largest was ~33.3 μm^3 (Fig. 6*C* and *SI Appendix*, Fig. S11). Interestingly, the overall shape and proportions appeared to be similar despite these size differences. To rigorously determine how the proportions of compartments and regions in LROs scale with size, we analyzed correlations between the volumes of the LysoTracker region, zinc region, and expansion compartment and the total volume. In zinc excess and deficiency, the expansion compartment and LysoTracker region positively correlated with total volume, indicating that LROs have a similar composition regardless of size (*SI Appendix*, Fig. S13). In zinc-replete conditions, only the LysoTracker region positively correlated with total volume (*SI Appendix*, Fig. S13).

Vesicles Appear to Deliver Zinc Transporters to LROs, thereby Increasing the Volume of the Expansion Compartment. In zinc excess, we frequently observed small, spherical vesicles that were positive for CDF-2 adjacent to or fusing with the expansion compartment. In zinc deficiency, we occasionally observed such vesicles (Fig. 7*C*). Based on these observations, we propose that vesicle fusion may deliver CDF-2 to LROs in zinc excess and may be the source of the increase in the

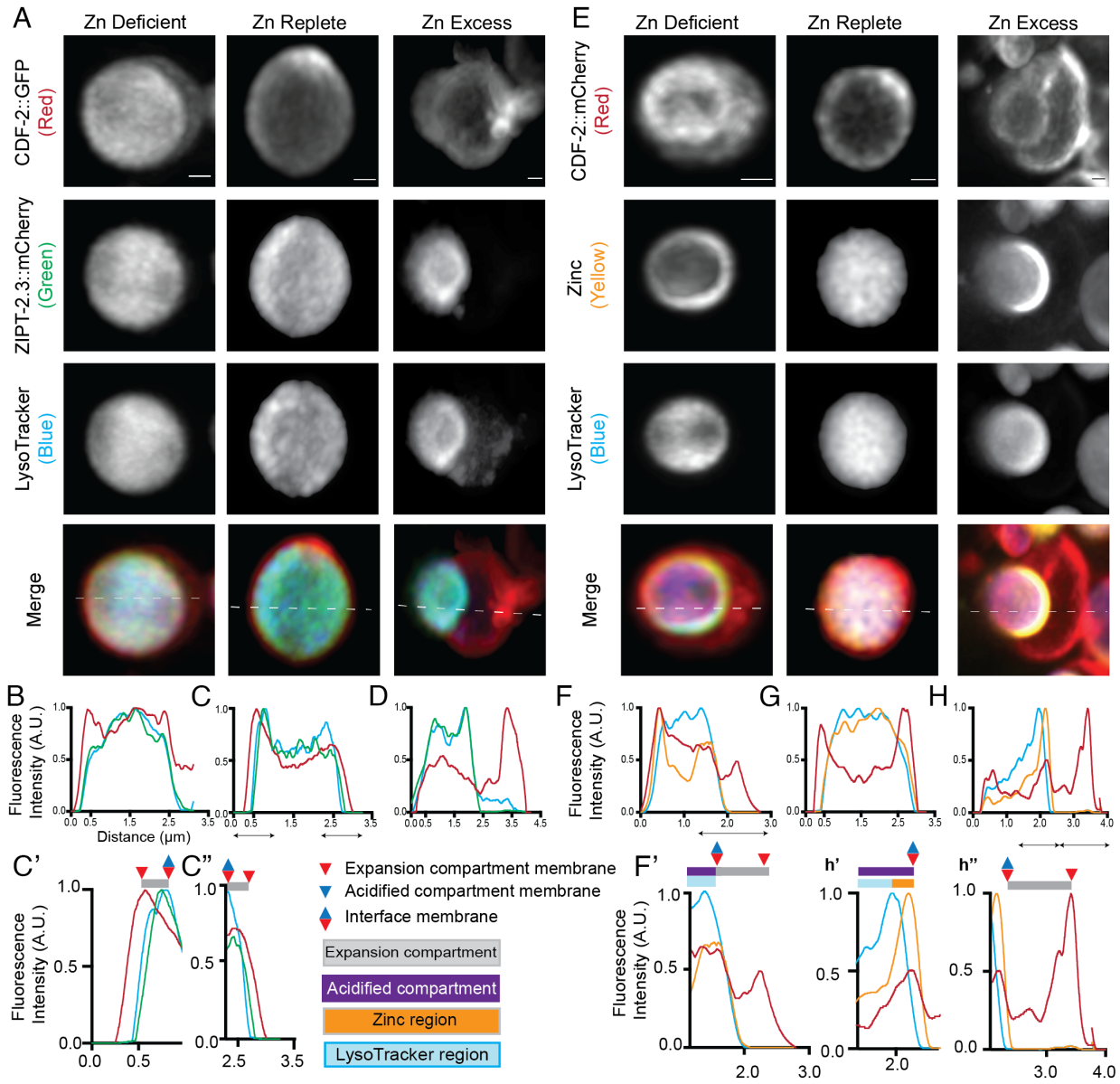

Fig. 5. Super-resolution microscopy reveals that LROs are composed of an acidified and an expansion compartment. (*A*) Transgenic L4 stage animals expressing CDF-2::GFP (arbitrary color red) and ZIPT-2.3::mCherry (arbitrary color green) were cultured for 16 h in LysoTracker Blue (arbitrary color blue) in either standard medium (Zn replete), 50 μM TPEN (Zn deficient), or 200 μM supplemental zinc (Zn excess). Individual LROs were imaged by super-resolution microscopy for green, red, and blue fluorescence, and a MIP is displayed. (Scale bar, 0.5 μm.) (*B–D*) A line scan was performed, indicated by the dashed white line on the merge image. For each color, the highest value was set equal to 1.0 arbitrary units (AU), and other values were normalized. (*C′* and *C″*) Enlargements of specific regions indicated by black double-sided arrows. Annotations above indicate positions of membranes (triangles), compartments (purple and gray rectangles), and regions (blue and orange rectangles) as defined in the key between *C″* and *F′*. (*E–H*) Transgenic L4 stage animals expressing CDF-2::mCherry (arbitrary color red) were cultured for 16 to 20 h in LysoTracker Blue (arbitrary color blue) and the zinc dye FluoZin-3 AM (arbitrary color yellow). Culture conditions, imaging, line scan analysis, and enlargements in *F′*, *H′*, and *H″* are as described for panels *A–D*.

expansion compartment volume. Similarly, we propose that vesicle fusion may be responsible for delivering ZIPT-2.3 to LROs in zinc deficiency and may be the source of the increase in the expansion compartment volume. The process seems to be robust in zinc excess conditions, resulting in the appearance of many vesicles and a dramatic increase in the volume of the expansion compartment; the process is less robust in zinc deficiency, since fewer vesicles were observed and changes in the expansion compartment volume are subtler (Fig. 7*A*). Static images do not rigorously establish the mechanism of this dynamic process, and an alternative model is that removal of expansion compartment membrane is reduced in zinc excess and deficiency, resulting in a volume increase.

Based on these observations and previous studies of zinc-regulated transcription, we propose an integrated model of zinc homeostasis (Fig. 7*B*). In zinc excess, zinc binds the HIZR-1 LBD, and HIZR-1 translocates to the nucleus where its DBD interacts with the HZA enhancer, increasing *cdf-2* transcription. By contrast, transcription of *zipt-2.3* is decreased by an unknown mechanism. Increased levels of *cdf-2* transcripts result in increased translation of CDF-2 protein in the endoplasmic reticulum and the generation of vesicles that fuse with the expansion compartment of LROs. Vesicle fusion adds membrane and increases the volume of the expansion compartment; increased levels of CDF-2 promote zinc transport and detoxification, and zinc is concentrated in the zinc region (Fig. 7 *B*, *Lower*). In zinc-replete conditions, transcription of *cdf-2* and *zipt-2.3* are balanced, and only a small number of vesicles fuse with LROs, so the expansion compartment is contracted (Fig. 7 *B*, *Middle*). In zinc deficiency, the LZA enhancer is activated, leading to increased levels of *zipt-2.3* transcripts. By contrast, the *cdf-2*

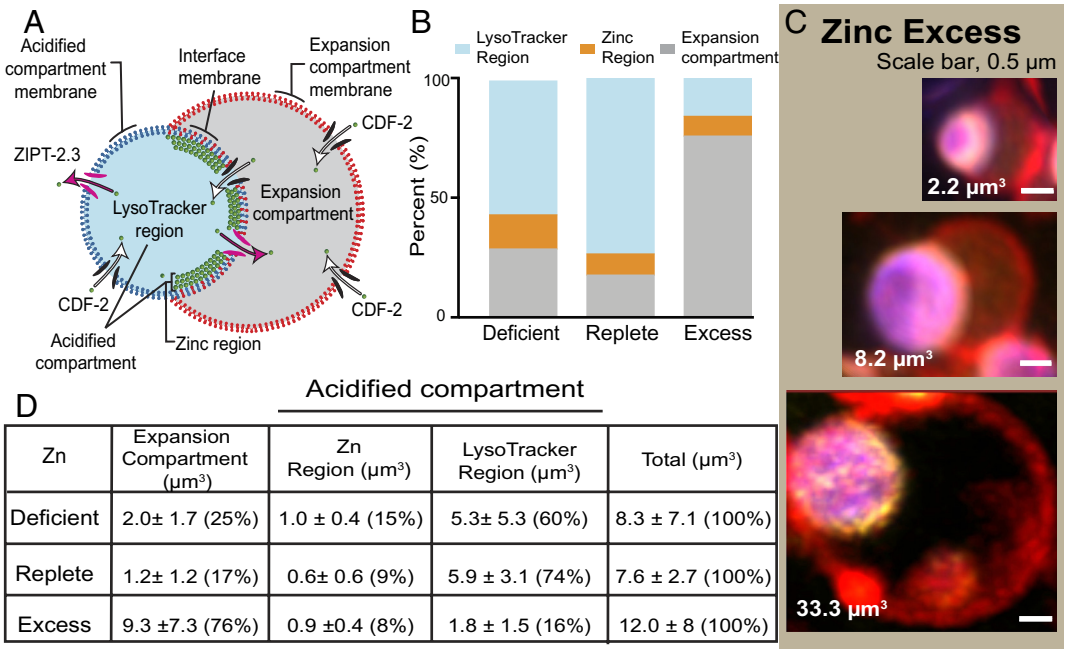

D

Acidified compartment

Zn	Expansion Compartment (µm³)	Zn Region (µm³)	LysoTracker Region (µm³)	Total (µm³)
Deficient	2.0± 1.7 (25%)	1.0 ± 0.4 (15%)	5.3± 5.3 (60%)	8.3 ± 7.1 (100%)
Replete	1.2± 1.2 (17%)	0.6± 0.6 (9%)	5.9 ± 3.1 (74%)	7.6 ± 2.7 (100%)
Excess	9.3 ±7.3 (76%)	0.9 ±0.4 (8%)	1.8 ± 1.5 (16%)	12.0 ± 8 (100%)

Fig. 6. LROs dynamically respond to changing cytosolic zinc levels. (*A*) Model of an LRO in zinc-excess conditions. Compartments, regions, and membranes are labeled. CDF-2 and ZIPT-2.3 proteins are black/white or pink arrows, respectively. (*B*) Transgenic L4 stage animals expressing CDF-2::mCherry were cultured for 16 to 20 h in LysoTracker Blue and the zinc dye FluoZin-3 AM in either standard medium (Zn replete), 50 µM TPEN (Zn deficient), or 200 µM supplemental zinc (Zn excess). Individual LROs were imaged by super-resolution microscopy for green, red, and blue fluorescence. The volumes of the LysoTracker region, zinc region, and expansion compartment were quantified as described in *SI Appendix*, Fig. S5. (*C*) Merge images of LROs from animals cultured in zinc excess illustrate volume variation. (Scale bar, 0.5 µm.) The same LROs are shown in *SI Appendix*, Fig. S11. (*D*) Volumes of the expansion compartment, zinc region, LysoTracker region, and total LRO were determined as described in panel *B*. Values are average ± SD, and percent is the fraction of the total volume. N = 11 deficient LROs, 12 replete LROs, and 11 excess LROs.

promoter is repressed by an unknown mechanism. Increased levels of *zipt-2.3* transcripts result in increased translation of ZIPT-2.3 protein in the endoplasmic reticulum and the generation of vesicles that fuse with the expansion compartment of LROs. Vesicle fusion enlarges the expansion compartment slightly, and increased levels of ZIPT-2.3 promote zinc export (Fig. 7 *B*, *Upper*).

Discussion

Reciprocal Regulation of CDF-2 and ZIPT-2.3 Is a Fundamental Mechanism of Zinc Homeostasis. The lysosome is emerging as an evolutionarily conserved site of zinc storage in eukaryotes, including the vacuole of yeast (26), acidocalcisomes of Chlamydomonas (27, 28), LROs in intestinal cells of worms (13), and zincosomes in mammals (3, 29, 30). In *C. elegans*, CDF-2 transports zinc from cytosol to lumen of LROs (13). Here, we show that ZIPT-2.3 transports zinc from the lumen back into the cytosol. This conclusion is based on ZIPT-2.3 transport activity in cultured cells, specific localization of ZIPT-2.3 to the acidified compartment of LROs, and genetic analysis showing *zipt-2.3* is necessary to release zinc stored in LROs. The identification of CDF-2 and ZIPT-2.3 as the pair of transporters that control zinc storage and release from LROs is an important advance in understanding zinc homeostasis. Fourteen ZIPT proteins are present in *C. elegans* (14, 15); Sue et al. (2022) reported that ZIPT-2.4 localizes to the germline and vesicular-like structures in the intestine (31), raising the possibility that it also functions in zinc homeostasis in LROs.

ZIPT-2.3 and CDF-2 display reciprocal regulation in response to low and high zinc conditions, identifying a fundamental mechanism for directional flow. In excess zinc, HIZR-1 (9) translocates to the nucleus and activates transcription of *cdf-2*, increasing zinc storage capacity in LROs. Here, we show excess zinc also reduced levels of *zipt-2.3* mRNA, reducing zinc release capacity. The mechanism of transcriptional repression by high zinc is unknown and represents an important question for future studies. We propose that high levels of CDF-2 and low levels of ZIPT-2.3 are responsible for the net flow of zinc from the cytosol into the lumen of LROs in zinc excess.

During zinc deficiency, an unknown mechanism activates the LZA enhancer, resulting in high levels of *zipt-2.3* transcript and increased capacity for zinc mobilization from LROs. Chapman et al. (2019) reported that transcription factor KLF-3 mediates *zipt-2.3* expression, but the relationship to the LZA enhancer is unknown (20). Here, we show zinc deficiency also results in reduced levels of *cdf-2* mRNA, reducing zinc storage capacity. The mechanism of transcriptional repression by low zinc is unknown, laying the foundation for future studies. We propose that high levels of ZIPT-2.3 and low levels of CDF-2 are responsible for the net flow of zinc from the lumen of LROs into the cytosol during zinc deficiency.

Transcriptional control of CDF and ZIP proteins is well documented in yeast. In zinc deficiency, the zinc-responsive transcription factor Zap1 becomes active, leading to the elevated expression of the vacuolar zinc transporters Zrt3 and Zrc1, and the ER transporter Zrg17 (32, 33). Zrt3 is a ZIP protein that localizes to the vacuole and releases zinc (30). In mammals, many ZNT and ZIP family members are reported to localize to the ER, Golgi, and lysosome in various cell types; however, little is known about pairs of ZNT and ZIP proteins that localize to the same lysosome. ZIP3 (34) and ZIP8 (35) localize to lysosomes, suggesting that these proteins may release stored zinc. The zinc exporter ZNT2 localizes to lysosomes (36) and regulates zinc storage during mammary gland involution (37). ZNT3 and ZNT4 co-localize with LAMP-1, an endolysosomal marker, suggesting that they promote zinc storage in lysosomes (38, 39). ZNT4 cooperates with TRPML1, a zinc importer, to regulate zinc flow between the cytosol and the lysosome (40),

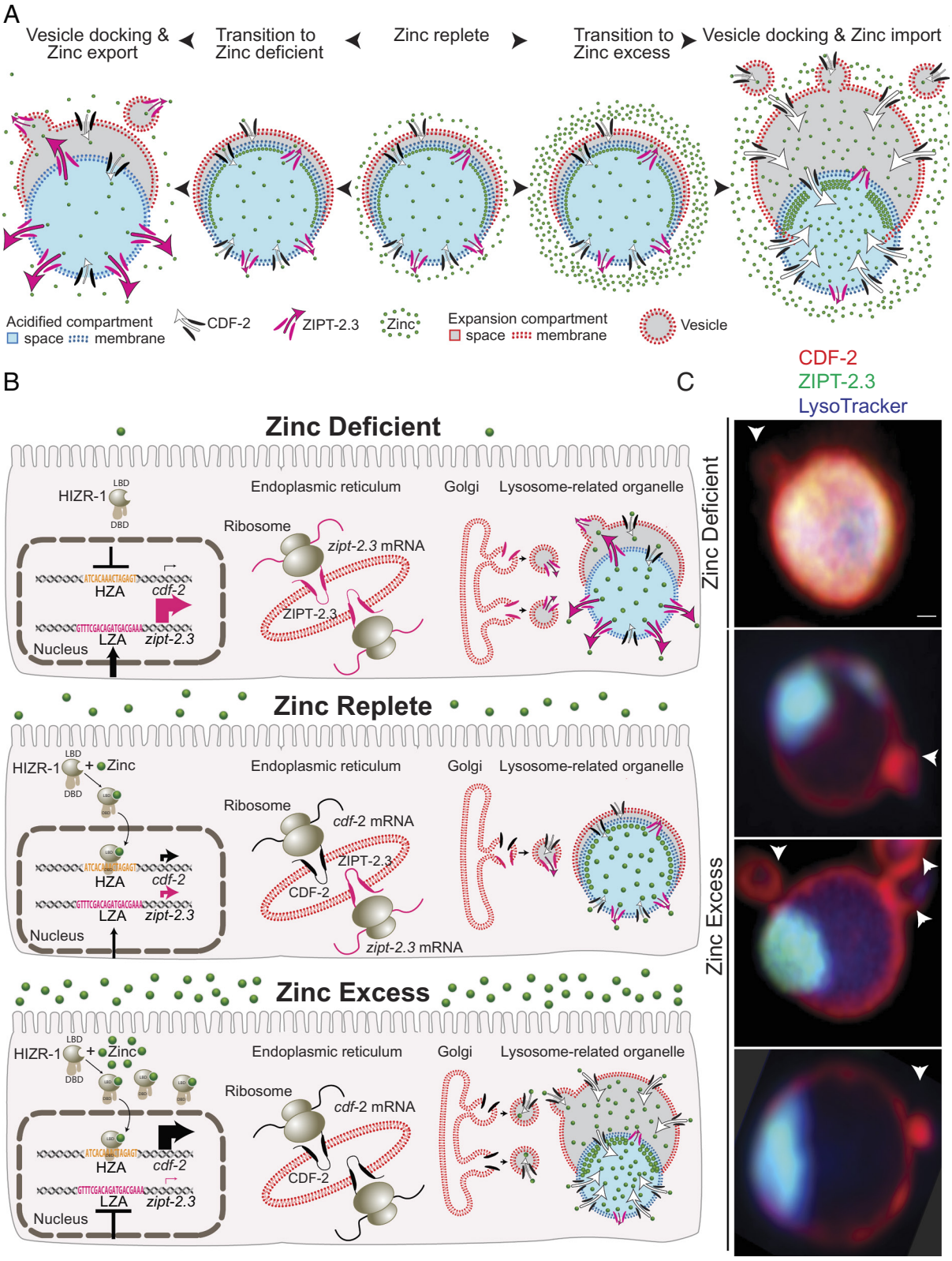

Fig. 7. Vesicle fusion may enlarge the expansion compartment and deliver CDF-2 and ZIPT-2.3. (*A*) Model of the morphological transition of LROs and changes in transporter levels during the shift from zinc replete to excess or deficiency. (*B*) Model of zinc homeostasis in zinc-deficient (*Upper*), -replete (*Middle*), and -excess (*Lower*) conditions. The HIZR-1 transcription factor, composed of a LBD and a DBD, acts through the HZA enhancer to regulate expression of *cdf-2*; an undefined system for sensing low zinc acts through the LZA enhancer to regulate expression of *zipt-2.3*. mRNA is translated in the endoplasmic reticulum, and Golgi-derived vesicles deliver CDF-2 (black) and ZIPT-2.3 (magenta) protein to LROs, enlarging the expansion compartment in zinc-excess and -deficient conditions. (*C*) Transgenic L4 stage animals expressing CDF-2::GFP (arbitrary color red) and ZIPT-2.3::mCherry (arbitrary color green) were cultured for 16 h in LysoTracker Blue (arbitrary color blue) in either 50 μM TPEN (Zn deficient) or 200 μM supplemental zinc (Zn excess). Individual LROs were imaged by super-resolution microscopy for green, red, and blue fluorescence—these images are maximum intensity projections of a three-color merge. (Scale bar, 0.5 μm.) White arrow heads indicate CDF-2 positive vesicles in close proximity to the expansion compartment—some appear to be fusing with the expansion compartment membrane.

suggesting that this is another type of regulation for zinc storage and release.

LROs contain a dynamic expansion compartment. Roh et al. (2012) showed LROs adopt a bilobed morphology in high zinc, but the structure was not well defined (13). Here, we used super-resolution microscopy, new markers, and a wider range of zinc concentrations to advance understanding of the bilobed morphology and lysosome remodeling. Our results indicate that LROs in intestinal cells are composed of an acidified compartment that stains with LysoTracker, CDF-2, and ZIPT-2.3, and an expansion compartment that stains with CDF-2 but not LysoTracker or ZIPT-2.3. This raises the fascinating question of how these two membrane-bound compartments acquire and sustain different compositions of transmembrane proteins. The expansion compartment is dynamic—it increases in volume dramatically in high zinc, consistent with the results of Roh et al. (13). Furthermore, here we show that it increases in volume moderately in low zinc, indicating that remodeling occurs in both zinc extremes. Surprisingly, the expansion compartment is also present in zinc-replete conditions, but it is contracted and difficult to appreciate; it can be visualized with super-resolution microscopy, whereas it was not apparent with standard confocal microscopy.

In high zinc, the expansion compartment is often shaped like a hemisphere that appears to be attached to the acidified compartment. Hemisphere formation has been reported in yeast vacuoles, but it is a transient state (41) that facilitates selective protein degradation (42). An alternative model is that the expansion compartment completely surrounds the acidified compartment; this might occur by invagination, similar to formation of multivesicular bodies (43). This model predicts that line scans will always encounter the expansion compartment membrane before the acidified compartment membrane. However, our line scans often encountered the acidifed compartment first, indicating that in at least some LROs, the acidified compartment membrane contacts the cytosol rather than being completely surrounded by the expansion compartment membrane. Our data do not resolve the precise relationship between the two membrane compartments. The cartoons of LROs in Figs. 6 and 7 were drawn to look like typical LROs but are not meant to specifiy the detailed membrane structure; future studies are needed to distinguish these alternative models.

We propose that dynamic growth of the expansion compartment in high and low zinc is driven by vesicle fusion. In zinc excess, we frequently observed vesicles that appear to be fusing with the expansion compartment or were positioned close to it. This model is appealing because it explains the source of the membrane that allows the expansion compartment to increase in volume. However, our static images can only be used to infer dynamic processes. Alternative models are that vesicles are undergoing fission or are close to the expansion compartment by coincidence. Future studies, such as video recordings, are necessary to directly address the mechanisms of dynamic change in LROs.

The acidified compartment function is well established—the low pH environment promotes the activity of enzymes that degrade macromolecules for nutrient recycling. Our results document the existence of a dynamic expansion compartment, raising a new question: What is the function of this compartment? We propose that the expansion compartment is a mechanism to promote rapid transitions in the ratio of zinc transporters without disturbing the acidified compartment. According to this model, in zinc excess, the cell must increase the ratio of CDF-2 to ZIPT-2.3 on the membrane of LROs. This is accomplished by reciprocal regulation of transcription, which increases *cdf-2* levels and decreases *zipt-2.3* levels, followed by delivery of vesicles with the new ratio of transporters to the expansion compartment. Because fusion of the new vesicles occurs at the expansion compartment, the acidified compartment is protected from fusion to vesicles that are not acidified. Conversely, in zinc deficiency, reciprocal transcriptional regulation increases *zipt-2.3* levels and decreases *cdf-2* levels, so newly synthesized vesicles that fuse to the expansion compartment will begin to shift the transporter ratio to favor zinc release.

Metal storage in LROs. To determine the volume of the zinc region, we measured and then calculated the area stained with fluorescent zinc dye. FluoZin-3 AM detects "labile" zinc that is chelatable by the dye, but not total zinc. The calculated volumes were 0.6 ± 0.6 μm^3 in replete, 0.9 ± 0.4 μm^3 in excess, and 1.0 ± 0.4 μm^3 in deficient; there was no statistical difference between these values or between these volumes calculated as a percent of total LRO volume. We did not quantify zinc levels in individual LROs. The overall amount of FluoZin-3 AM staining in the intestine decreases in zinc deficiency compared to excess (13). These results indicate that the volume of the zinc region in individual LROs does not correlate well with the overall amount of zinc stored in the intestine. One interpretation is that the number of LROs is reduced in zinc deficiency compared to excess; thus, while the volume of zinc regions in individual LROs is not altered significantly, the overall volume of zinc regions is smaller in deficiency due to a smaller number of LROs. Alternatively, the volume of the zinc region may not correlate with the amount of zinc stored. Future studies that quantify total zinc in individual lysosomes using X-ray fluorescence microscopy would help distinguish these alternative models.

Our results show that labile zinc is concentrated in the acidified compartment lumen; however, CDF-2 localizes to the expansion compartment membrane, suggesting that zinc may also be transported into the expansion compartment lumen. One possibility is that zinc in the expansion compartment is not visualized by FluoZin-3 AM, either because the dye is not located in the expansion compartment or this zinc is tightly bound and not labile. Alternatively, zinc that enters the expansion compartment may be rapidly transported to the acidified compartment. Another possibility is that zinc does not enter the expansion compartment effectively because CDF-2 activity on that membrane is low. CDF-2 is part of the SLC30A family, and some members are H+ antiporters (44). If CDF-2 is also a H+ antiporter, then it might be highly active on the acidified compartment membrane due to the low pH of the lumen, whereas it might be less active on the expansion compartment membrane due to the higher pH of that lumen. Thus, localization to compartments with different pH may be another regulatory mechanism to control CDF-2 activity.

The anion that balances the Zn^{2+} charge in the LRO is unknown; anthranillic acid (45) has been reported to exist in intestinal LROs and may be a candidate. An interesting possibility is that the anion is transported in parallel with zinc, and the anion transporter may be regulated by the high and low-zinc homeostasis pathways.

Here, we focus on zinc, but the LRO may also store other metals. Chun et al. (2017) showed that LROs in intestinal cells of *C. elegans* store copper, and the copper transporter CUA-1 re-localizes from the intestinal basolateral membrane to LROs during excess copper exposure (46). While LROs store both copper and zinc, it is unknown whether these metals are stored in the same location and whether copper storage involves dynamic changes in the expansion compartment. LROs in Chlamydomonas, known as acidocalcisomes, are also a site for metal mobilization and sensitive to zinc levels in the cell. Zinc deficiency in Chlamydomonas results in iron and copper hyperaccumulation in acidocalcisomes (27, 47). Our results establish the foundation for understanding how the structure of LROs facilitates multiple activities including degradation of

macromolecules and storage of essential nutrients such as zinc and copper.

Experimental Procedures Summary

Plasmid DNA construction and transgenic strain generation used standard *C. elegans* techniques. Worm growth was measured after 3 d using microscopy. Zinc shift assays were performed with FluoZin-3 AM. Quantitative real-time PCR was performed using standard methods (14). Zinc uptake assays were performed using HEK293T cells based on methods described by Gaither and Eide (48). Spinning-disk microscopy and super-resolution microscopy were performed on live animals. Comparisons of data were performed using the two-tailed unpaired Student's *t* test or a 2-way ANOVA, and a *P* value <0.05 was considered significant. Pearson correlations were first analyzed by 1-way ANOVA; when $P < 0.05$, data were further analyzed by a student's *t* test. See *SI Appendix* for detailed methods.

Data, Materials, and Software Availability. All study data are included in the article and/or *SI Appendix*.

ACKNOWLEDGMENTS. We thank Laura Kyro for graphics and Suzanne Pfeffer for advice. pCFJ90-Pmyo-2::mCherry::*unc-54*utr was a gift from Erik Jorgensen (Addgene plasmid #19327). NIH R01GM068598 to K.K. C.-H.T. was a scholar of the McDonnell International Scholars Academy. A.D.M. was supported by the T32HLHL7081 and 1K99GM146016-01. Confocal/super-resolution microscopes were purchased with support from the Office of Research Infrastructure Programs, part of the NIH Office of the Director (grant OD021629).

Author affiliations: [a]Department of Developmental Biology, Washington University School of Medicine, St. Louis, MO 63110

Author contributions: A.D.M., N.D., C.-H.T., and K.K. designed research; A.D.M., N.D., C.-H.T., D.H., J.K., Z.P., and D.L.S. performed research; N.D. and C.C. contributed new reagents/analytic tools; A.D.M., N.D., C.-H.T., D.H., J.K., Z.P., and K.K. analyzed data; and A.D.M., N.D., and K.K. wrote the paper.

The authors declare no competing interest.

This article is a PNAS Direct Submission.

1. W. Maret, Y. Li, Coordination dynamics of zinc in proteins. *Chem. Rev.* **109**, 4682–4707 (2009).
2. K. A. McCall, C. Huang, C. A. Fierke, Function and mechanism of zinc metalloenzymes. *J. Nutr.* **130**, 1437S–1446S (2000).
3. D. Beyersmann, H. Haase, Functions of zinc in signaling, proliferation and differentiation of mammalian cells. *Biometals* **14**, 331–341 (2001).
4. C. Andreini, L. Banci, I. Bertini, A. Rosato, Counting the zinc-proteins encoded in the human genome. *J. Proteome Res.* **5**, 196–201 (2006).
5. J. L. Vinkenborg *et al.*, Genetically encoded FRET sensors to monitor intracellular Zn2+ homeostasis. *Nat. Methods* **6**, 737–740 (2009).
6. T. Kimura, T. Kambe, The functions of metallothionein and ZIP and ZnT transporters: An overview and perspective. *Int. J. Mol. Sci.* **17**, 336 (2016).
7. B. J. Earley, A. D. Mendoza, C. H. Tan, K. Kornfeld, Zinc homeostasis and signaling in the roundworm C. elegans. *Biochim. Biophys. Acta Mol. Cell Res.* **1868**, 118882 (2021).
8. N. Dietrich, C. H. Tan, C. Cubillas, B. J. Earley, K. Kornfeld, Insights into zinc and cadmium biology in the nematode Caenorhabditis elegans. *Arch Biochem. Biophys.* **611**, 120–133 (2016).
9. K. Warnhoff *et al.*, The nuclear receptor HIZR-1 uses zinc as a ligand to mediate homeostasis in response to high zinc. *PLoS Biol.* **15**, e2000094 (2017).
10. H. C. Roh *et al.*, A modular system of DNA enhancer elements mediates tissue-specific activation of transcription by high dietary zinc in C. elegans. *Nucleic Acids Res.* **43**, 803–816 (2015).
11. H. C. Roh *et al.*, ttm-1 encodes CDF transporters that excrete zinc from intestinal cells of C. elegans and act in a parallel negative feedback circuit that promotes homeostasis. *PLoS Genet.* **9**, e1003522 (2013).
12. N. Shomer *et al.*, Mediator subunit MDT-15/MED15 and nuclear receptor HIZR-1/HNF4 cooperate to regulate toxic metal stress responses in Caenorhabditis elegans. *PLoS Genet.* **15**, e1008508 (2019).
13. H. C. Roh, S. Collier, J. Guthrie, J. D. Robertson, K. Kornfeld, Lysosome-related organelles in intestinal cells are a zinc storage site in C. elegans. *Cell Metab.* **15**, 88–99 (2012).
14. N. Dietrich, D. L. Schneider, K. Kornfeld, A pathway for low zinc homeostasis that is conserved in animals and acts in parallel to the pathway for high zinc homeostasis. *Nucleic Acids Res.* **45**, 11658–11672 (2017).
15. Y. Zhao *et al.*, The zinc transporter ZIPT-7.1 regulates sperm activation in nematodes. *PLoS Biol.* **16**, e2005069 (2018).
16. S. Yin, Q. Qin, B. Zhou, Functional studies of Drosophila zinc transporters reveal the mechanism for zinc excretion in Malpighian tubules. *BMC Biol.* **15**, 12 (2017).
17. A. Qiu, M. Shayeghi, C. Hogstrand, Molecular cloning and functional characterization of a high-affinity zinc importer (DrZIP1) from zebrafish (Danio rerio). *Biochem. J.* **388**, 745–754 (2005).
18. R. E. Dempski, The cation selectivity of the ZIP transporters. *Curr. Top Membr.* **69**, 221–245 (2012).
19. N. Grotz *et al.*, Identification of a family of zinc transporter genes from Arabidopsis that respond to zinc deficiency. *Proc. Natl. Acad. Sci. U.S.A.* **95**, 7220–7224 (1998).
20. E. M. Chapman *et al.*, A conserved CCM complex promotes apoptosis non-autonomously by regulating zinc homeostasis. *Nat. Commun.* **10**, 1791 (2019).
21. D. E. Davis *et al.*, The cation diffusion facilitator gene cdf-2 mediates zinc metabolism in Caenorhabditis elegans. *Genetics* **182**, 1015–1033 (2009).
22. G. J. Hermann *et al.*, Genetic analysis of lysosomal trafficking in Caenorhabditis elegans. *Mol. Biol. Cell* **16**, 3273–3288 (2005).
23. C. Morris *et al.*, Function and regulation of the Caenorhabditis elegans Rab32 family member GLO-1 in lysosome-related organelle biogenesis. *PLoS Genet.* **14**, e1007772 (2018).
24. L. Voss *et al.*, An ABCG transporter functions in rab localization and lysosome-related organelle biogenesis in Caenorhabditis elegans. *Genetics* **214**, 419–445 (2020).
25. B. Chazotte, Labeling lysosomes in live cells with LysoTracker. *Cold Spring Harb. Protoc.* **2011**, pdb.prot5571 (2011).
26. C. Simm *et al.*, Saccharomyces cerevisiae vacuole in zinc storage and intracellular zinc distribution. *Eukaryot. Cell* **6**, 1166–1177 (2007).
27. S. Schmollinger *et al.*, Single-cell visualization and quantification of trace metals in Chlamydomonas lysosome-related organelles. *Proc. Natl. Acad. Sci. U.S.A.* **118**, e2026811118 (2021).
28. C. E. Blaby-Haas, S. S. Merchant, Lysosome-related organelles as mediators of metal homeostasis. *J. Biol. Chem.* **289**, 28129–28136 (2014).
29. H. Haase, D. Beyersmann, Uptake and intracellular distribution of labile and total Zn(II) in C6 rat glioma cells investigated with fluorescent probes and atomic absorption. *Biometals* **12**, 247–254 (1999).
30. D. J. Eide, Zinc transporters and the cellular trafficking of zinc. *Biochim. Biophys. Acta* **1763**, 711–722 (2006).
31. A. C. Sue, S. M. Wignall, T. K. Woodruff, T. V. O'Halloran, Zinc transporters ZIPT-2.4 and ZIPT-15 are required for normal C. elegans fecundity. *J. Assist Reprod. Genet.* **39**, 1261–1276 (2022).
32. D. J. Eide, Homeostatic and adaptive responses to zinc deficiency in Saccharomyces cerevisiae. *J. Biol. Chem.* **284**, 18565–18569 (2009).
33. A. J. Bird, S. Wilson, Zinc homeostasis in the secretory pathway in yeast. *Curr. Opin. Chem. Biol.* **55**, 145–150 (2020).
34. L. Huang, C. P. Kirschke, Y. Zhang, Decreased intracellular zinc in human tumorigenic prostate epithelial cells: A possible role in prostate cancer progression. *Cancer Cell Int.* **6**, 10 (2006).
35. T. B. Aydemir, J. P. Liuzzi, S. McClellan, R. J. Cousins, Zinc transporter ZIP8 (SLC39A8) and zinc influence IFN-gamma expression in activated human T cells. *J. Leukoc. Biol.* **86**, 337–348 (2009).
36. V. Lopez, S. L. Kelleher, Zinc transporter-2 (ZnT2) variants are localized to distinct subcellular compartments and functionally transport zinc. *Biochem. J.* **422**, 43–52 (2009).
37. S. R. Hennigar, Y. A. Seo, S. Sharma, D. I. Soybel, S. L. Kelleher, ZnT2 is a critical mediator of lysosomal-mediated cell death during early mammary gland involution. *Sci. Rep.* **5**, 8033 (2015).
38. J. M. Falcon-Perez, E. C. Dell'Angelica, Zinc transporter 2 (SLC30A2) can suppress the vesicular zinc defect of adaptor protein 3-depleted fibroblasts by promoting zinc accumulation in lysosomes. *Exp. Cell Res.* **313**, 1473–1483 (2007).
39. H. Lee, J. Y. Koh, Roles for H(+) /K(+) -ATPase and zinc transporter 3 in cAMP-mediated lysosomal acidification in bafilomycin A1-treated astrocytes. *Glia* **69**, 1110–1125 (2021).
40. I. Kukic, J. K. Lee, J. Coblentz, S. L. Kelleher, K. Kiselyov, Zinc-dependent lysosomal enlargement in TRPML1-deficient cells involves MTF-1 transcription factor and ZnT4 (Slc30a4) transporter. *Biochem. J.* **451**, 155–163 (2013).
41. L. Wang, E. S. Seeley, W. Wickner, A. J. Merz, Vacuole fusion at a ring of vertex docking sites leaves membrane fragments within the organelle. *Cell* **108**, 357–369 (2002).
42. E. K. McNally, M. A. Karim, C. L. Brett, Selective lysosomal transporter degradation by organelle membrane fusion. *Dev. Cell* **40**, 151–167 (2017).
43. R. C. Piper, D. J. Katzmann, Biogenesis and function of multivesicular bodies. *Annu. Rev. Cell Dev. Biol.* **23**, 519–547 (2007).
44. Y. Golan, R. Alhadeff, A. Warshel, Y. G. Assaraf, ZnT2 is an electroneutral proton-coupled vesicular antiporter displaying an apparent stoichiometry of two protons per zinc ion. *PLoS Comput. Biol.* **15**, e1006882 (2019).
45. C. Coburn *et al.*, Anthranilate fluorescence marks a calcium-propagated necrotic wave that promotes organismal death in C. elegans. *PLoS Biol.* **11**, e1001613 (2013).
46. H. Chun *et al.*, The intestinal copper exporter CUA-1 is required for systemic copper homeostasis in Caenorhabditis elegans. *J. Biol. Chem.* **292**, 1–14 (2017).
47. A. Hong-Hermesdorf *et al.*, Subcellular metal imaging identifies dynamic sites of Cu accumulation in Chlamydomonas. *Nat. Chem. Biol.* **10**, 1034–1042 (2014).
48. L. A. Gaither, D. J. Eide, Functional expression of the human hZIP2 zinc transporter. *J. Biol. Chem.* **275**, 5560–5564 (2000).